Catal Lett (2009) 129:336–343
DOI 10.1007/s10562-009-9848-7

On the La–Cr–O Phase Change During Methane Catalytic Combustion Investigated with in situ HT-XRD

A. Kaddouri · S. Ifrah · G. Bergeret

Received: 30 June 2008 / Accepted: 7 January 2009 / Published online: 23 January 2009

Abstract La_2CrO_6 (Cr6), $LaCrO_3$ (Cr3), $LaCrO_3$–La_2CrO_6 (Cr6–Cr3) and $LaCrO_3$–La_2O_3 (Cr3-L) catalysts were synthesised and investigated with in situ X-ray diffraction (ISXRD) during methane catalytic combustion in order to characterise the solid phases present under reactants and to determine the effect of chromium oxidation state on the catalytic activity. Methane conversion was evaluated over a temperature range of 300–800 °C, using oxygen-to-methane ratio of 4 and GHSV of 8,000 h^{-1}. The TPR provided information about the oxygen depletion temperatures characteristic of lattice oxygen mobility in the samples and ISXRD results evidenced a cooperative effect of Cr3 and Cr6 phases at low temperatures (<725 °C) and of Cr3 and $LaCrO_4$ (Cr4) phases at high temperatures (>750 °C). The relative phase composition determined the oxygen activation capability and hence the corresponding activity for the oxidation of methane. It was observed that while direct and back Cr6 ↔ Cr4 transition temperatures were unaffected by Cr6 content in the samples, the methane conversion was strongly modified. This suggests that Cr^{3+}/Cr^{6+} and Cr^{3+}/Cr^{5+} species involved substantial modification of the surface chemistry which affected the catalytic activity. These results provide the first direct evidence of the presence of Cr4 metastable phase during methane combustion over La–Cr–O catalysts.

A. Kaddouri · S. Ifrah · G. Bergeret
Université de Lyon, 69622 Lyon, France

A. Kaddouri (✉) · S. Ifrah · G. Bergeret
CNRS, UMR 5256, IRCELYON, Institut de recherches sur la catalyse et l'environnement de Lyon, Université Lyon 1, 2 av. Albert Einstein, 69626 Villeurbanne, France
e-mail: akim.kaddouri@ircelyon.univ-lyon1.fr

Keywords La–Cr–O-system · In situ X-ray diffraction (ISXRD) characterisation · CH_4 combustion

1 Introduction

Perovskites-type oxides having high stability at high temperatures are suitable for several applications among which, as catalysts for the oxidation of hydrocarbons [1–4], olefins [5–7], carbon monoxide [8–10], for diesel soot abatement [11–13], and waste gas purification [14–16]. The good stability together with the intrinsic catalytic activity of perovskites has motivated continuous studies for purpose of improving their characteristics [17]. Most investigations were focused on the addition of various metal oxides to $LaCrO_3$, $LaMnO_3$, $LaFeO_3$ and $LaCoO_3$ perovskites. Among the binary perovskites, the oxygen stoichiometric $LaCoO_3$ has in several cases been mentioned as the most active [18, 19]. But the oxygen over-stoichiometric $LaMnO_{3+\delta}$ more frequently exhibits the highest activity [19, 20]. This has been attributed to its high thermal stability, the presence of manganese in two oxidation states (Mn^{3+}/Mn^{4+}) and large BET surface area. A number of detailed investigations showed that both the oxygen partial pressure and the synthesis temperature could be used to control the Mn^{3+}/Mn^{4+} ratio in $LaMnO_{3+\delta}$ [21–24]. High temperature synthesis led to samples with low over-stochiometry while low temperature synthesis yielded high cationic vacancy concentrations.

Numerous studies have been carried out for better understanding of the promoting effect of $LaCrO_3$ based perovskites in the oxidation process [25, 26]. It was described that for instance K substituted lanthanum chromium perovskite exhibits highest activity for soot diesel

abatement due to the presence of a great amount of chemisorbed α-oxygen with respect to the undoped perovskite [13]. Few reports have mentioned the effect of phase composition of La–Cr–O-systems on the catalytic performance in methane combustion [27] and very little is known about the effect of Cr^{3+}/Cr^{6+} or Cr^{3+}/Cr^{5+} ratios on the activity.

The development of techniques, which can provide structural information under in situ conditions, is strongly desired in heterogeneous catalysis [28, 29]. X-ray diffraction, among other techniques, gives the possibility of performing structural characterisation of the catalyst in its working environment [30]. To the best of our knowledge, the combustion of methane over lanthanum chromium perovskites-type oxides has never been investigated dynamically with in situ X-ray diffraction for the determination of chromium oxidation states in the samples, during catalytic tests, and for their correlation with catalytic activity.

The present study reports a structural and surface characterisation of the interaction of methane with La–Cr–O catalysts by using in situ X-ray diffraction and other physicochemical methods such as X-ray Photoelectron Spectroscopy (XPS) and temperature-programmed reduction coupled with mass spectrometry (TPR-MS).

The aim here is to bring the knowledge of the more subtle effects engendered by the variation, under reaction conditions, of the oxidation state of Cr (Cr^{3+}/Cr^{6+} or Cr^{3+}/Cr^{5+}) on the catalytic combustion of methane. The results of these physico chemical characterisations are discussed in relation to the exhibited catalytic performance of the Lanthanum–chromium oxides catalysts.

2 Experimental

2.1 Preparation of Catalysts

Reagents: $La(NO_3)_3{\cdot}6H_2O$, $Cr(NO_3)_3{\cdot}9H_2O$ (Aldrich Chemical) with 99.8% purity were used as received.

The preparation of La–Cr–O- catalysts involved a homogeneous aqueous solution containing the mixture of very soluble salts in a suitable ratio. The mixture was transferred in a 250 mL Pyrex beaker then the precipitation of lanthanum–chromium precursors occurred by progressive addition of ammonia (pH = 8.5) as precipitating agent. The product was transferred into a Parr autoclave and treated at 200 °C under autogeneous pressure for 24 h. The solid product recovered by centrifugation and filtration has repeatedly been washed with distilled water and then dried at 120 °C for 20 h. Finally the powder was heated at 900 °C leading to different phases composition; Cr3–Cr6 or Cr3-L depending on the atmosphere under which the thermal treatment was performed (oxygen or hydrogen, respectively). For comparison, both pure Cr3 and Cr6 were prepared too. The former was obtained either from a direct calcination of the precipitate at 700 °C/2 h in air (sample Cr3-A) [31] or after heating the same precipitate, previously treated hydrothermally (200 °C–20 atm–24 h), at 850 °C/62 h (sample Cr3-B). Cr6 was obtained from pelletised mixture of La_2O_3 and Cr_2O_3 and calcination in oxygen at 900 °C/2 h [32].

2.2 Characterisation

In situ X-ray diffraction (ISXRD) patterns were recorded with a Siemens D500 diffractometer using Cu Kα radiation ($\lambda = 1.5418$ Å) operated at 40 kV, 30 mA. The apparatus is equipped with BROOKS mass flow controllers allowing performing XRD analyses at high temperatures under oxidative or reductive atmospheres or in the presence of reactants (methane–oxygen mixture in N_2).

As the powder X-ray diffraction data were collected stepwise it would not be possible to collect data over a large 2θ range if the reaction speed was fast, so before the in situ chemical looping type reactions several diffraction experiments were run under various conditions (i.e. heating to 850 °C in inert, oxidative and reductive atmospheres) in order to ascertain a suitable 2θ range for the study and to find the optimum scan rate. The pattern were recorded from 10° to 70° in 2θ, with $\Delta 2\theta = 0.04°$. The detection limit for phase identification was 0.5%. A heating and cooling rate of 2 °C/min were used in all the experiments carried out.

Temperature-Programmed Reduction-Mass Spectrometry (TPR-MS) experiments (1% H_2 in He) were performed in a temperature range of 25–950 °C (heating rate: 20 °C/min) using 40 mg of catalyst and a QMS apparatus model Omnistar (Pfeiffer vacuum).

X-ray photoelectron spectroscopy (XPS) analyses were performed using a Riber SIA 200 spectrometer (Riber, Rueil Malmaison, France) using an aluminium (Al K_α = 1487 eV) X-ray source and a take-off angle of 65° with respect to the specimen surface. C*1 s* peak at a binding energy (BE) of 285.0 eV was used as an internal standard.

For ISXRD experiments gas mixture (1% CH_4–4% O_2–balance N_2) was passed through the cell while XRD patterns were collected. XRD patterns were assigned using the JCPDS database. Experiments were performed between ambient and 850 °C and one atmosphere pressure. About 0.05 to 0.1 g of sample (particles size of 10–20 μm, which represents a volume of ca. 0.9 $cm^3/g_{catalyst}$), was used in every experiment, each of which was conducted over 10 h. A flow rate of 75 $cm^3\ min^{-1}$ was used; flow rates of 50 and 25 $cm^3\ min^{-1}$ were also used for comparison.

The thermocouple, which was encased in inconel steel, was situated below the sample. This location was

downstream of the catalyst bed so that any reactions catalysed by the thermocouple sheath could not affect the environment of the catalyst. Hence it can be stated with confidence that X-ray diffraction patterns refer to working catalysts in a true reaction environment.

Control experiments with CH_4 performed in the absence of catalyst (blank experiments) showed only a small level of carbon oxides formation: about 0.15 vol% in the output stream, mainly CO_2. The onset temperature of homogeneous combustion was ca. 800 °C.

The reaction products were periodically sampled (5 min) and simultaneously analysed on line by Agilent micro-chromatographs equipped with high sensitivity (5 ppm) thermal conductivity detectors.

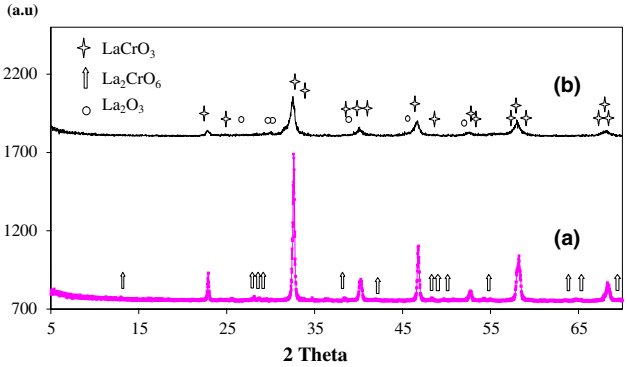

Fig. 1 X-ray diffraction patterns of lanthanum–chromium precursors calcined at 900 °C **a** under oxygen, **b** under hydrogen

3 Results and Discussion

3.1 XRD Analyses

The lanthanum chromium precursors were prepared in aqueous solution using successively conventional co-precipitation and hydrothermal treatment. Different atmospheres (oxygen, hydrogen) of calcination were used for converting the precursors into oxides. A variety of phase compositions of La–Cr–O were obtained depending on the heating atmosphere used. For instance 86%Cr3–14%Cr6 and 94% Cr3–6%L were obtained after 2 h heating at 900 °C under oxygen or hydrogen, respectively. Calcination of La–Cr–O precursors first under oxygen then under hydrogen lead to the same phase composition (94%Cr3–6%L) to that obtained after direct calcination of the same precursor under hydrogen. The XRD patterns, obtained at room temperature, of the samples calcined at 900 °C under oxygen or hydrogen are presented in Fig. 1. Phase composition was accurately estimated using Rietveld method for structure refinement. Table 1 reports the phase composition (XRD analysis) and the corresponding BET surface area of the biphasic catalysts together with pure Cr3 and Cr6 phases for comparison.

3.2 Temperature-programmed Reduction (TPR) Experiments

It is well known that, when a perovskite is heated at high temperature, oxygen vacancies can be formed. As thoroughly discussed in a review by Seyama (two types of chemisorbed oxygen species accompanied by related desorption peaks: a low temperature species, named α, desorbed in the 300–600 °C range, and a high temperature one, named β, desorbed at 600–900 °C [9].

The H_2-TPR profiles of the catalysts are presented in Fig. 2. For comparison, the profile of bulk Cr3 is also included in this figure. Under our experimental conditions, reduction of the 94% Cr3–6%La_2O_3 solid (not reported here) or pure Cr3 is not observed which is in agreement with literature reports [33]. The TPR pattern of the pure Cr6 is dominated by an important peak at ca. 650 °C. The TPR profile becomes smaller for both the 86%Cr3–14%Cr6 and 60%Cr3–40%Cr6 samples due to the presence of much less amounts of Cr6 in the sample. These peaks correspond to high temperature β-type oxygen species, desorbing in the temperature interval of 600–900 °C [34]. Consequently, we attributed the unique temperature peak observed for pure Cr6 (La_2CrO_6) and Cr3–Cr6 ($LaCrO_3$–La_2CrO_6) samples at 650 °C to the $La_2CrO_6 \rightarrow LaCrO_3 + 1/2La_2O_3 + 3/4O_2$ transformation ($Cr^{6+} \rightarrow Cr^{3+}$).

Total H_2 consumption registered for the samples is reported in Table 2. From the data it can be observed that the difference between theoretical and measured values depends on the amount of Cr6 present in the samples. This may be regarded as the effect of an incomplete reduction of the samples due to the interaction between Cr3 and Cr6. This interaction was found to be more important when the amount of the Cr6 phase was lower. On the contrary, when this was high this interaction was limited and the difference between calculated and measured H_2 was comparable to that observed for pure Cr6 phase. This is agreement with the onset of reduction temperature of the samples reported in Fig. 2.

3.3 XPS Investigations

In Fig. 3, the Cr_{2p} XPS spectrum of 86%Cr3–14%Cr6 sample is shown. Two Cr species can be found by curve deconvolution and they were assigned to Cr^{3+} and Cr^{6+}, whose BE were 573.57 eV for Cr^{3+} and 579.7 eV for Cr^{6+}. The ratio of the two Cr species (Cr^{3+}/Cr^{6+}) present on the catalytic surface was found to be 1.22. The surface concentration (% atom) of Cr species represents 17.8% (55% Cr^{3+}, and 45% Cr^{6+}) of the total surface composition.

Table 1 Phase composition and BET area versus preparation conditions

Synthesis method	Heating atmosphere	Phase composition after heating	Labelling	BET (m^2/g)
CoHC	Oxygen	86%$LaCrO_3$–14%La_2CrO_6	Cr3–Cr6	1.1
CoHC	Hydrogen	94% $LaCrO_3$–6%La_2O_3	Cr3-L	6.4
PC	Oxygen	La_2CrO_6	Cr6	3.1
CoC	Oxygen	$LaCrO_3$-A	Cr3-A	3.9
CoHCY	Oxygen	$LaCrO_3$-B	Cr3-B	0.9
DC	Oxygen	La_2O_3	L	6.7

CoHC Co-precipitation + hydrothermal (200 °C–20 atm–24 h) + calcination at 900 °C/2 h; *CoC* Co-precipitation + calcinations at 700 °C; *CoHCY* Co-precipitation + hydrothermal treatment (200 °C–20 atm–24 h) + calcination at 800 °C/62 h; *PC* Pelletized mixture of La_2O_3 and Cr_2O_3 calcined at 900 °C; *DC* Nitrates decomposition 800 °C/2 h

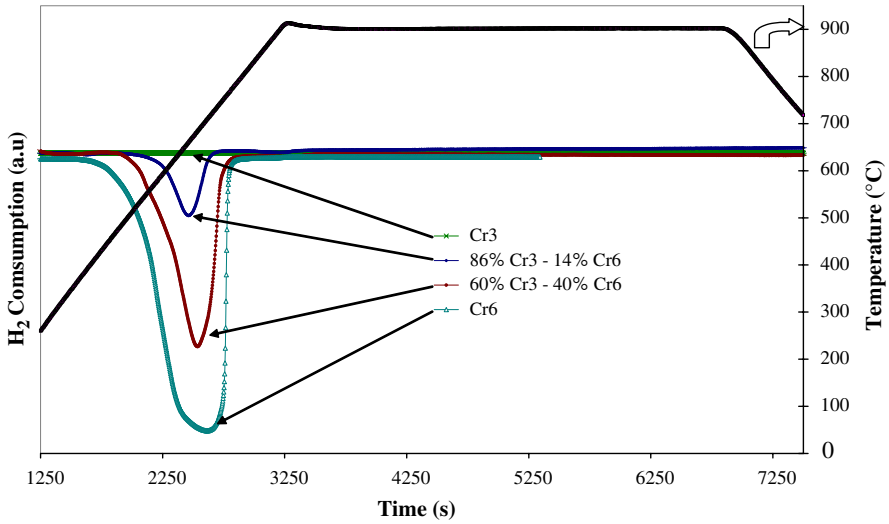

Fig. 2 TPR profiles of Cr3 and Cr6, 86%Cr3–14% Cr6 and 60% Cr3–40% Cr6

Table 2 Samples composition and H_2 consumption

Sample	Elements (w %)		H_2 consumption ($\times 10^{-3}$ mol/gcat)
	La	Cr	
Cr3 (theoretical)	58.14	21.76	–
Cr3-A (analysis)	57.46	21.88	No reduction
Cr3-B (analysis)	57.28	21.00	No reduction
94% Cr3–6% L (theoretical)	59.80	20.45	–
94% Cr3–6% L (analysis)	59.68	20.22	No reduction
86% Cr3–14% Cr6 (theoretical)	59.13	20.42	–
86% Cr3–14% Cr6 (analysis)	58.85	20.15	Measured **0.27** *expected 0.67* (based on * for 100% La_2CrO_6)
60% Cr3–40% Cr6 (theoretical)	60.98	17.94	–
60% Cr3–40% Cr6 (analysis)	60.38	17.42	Measured **1.29** *expected 1.62* (based on * for 100% La_2CrO_6)
Cr6 (theoretical)	65.24	12.21	**3.52** calculated from: $La_2CrO_6 + 3/2\ H_2 \rightarrow 1/2\ La_2O_3 + LaCrO_3 + 3/2\ H_2O$
Cr6 (analysis)	64.77	12.08	Measured **2.99***

For La and O elements this concentration was of 13.7 and 68.5%, respectively. Indeed with respect to Cr in Cr_2O_3 (576.6 eV) or in CrO_3 (579.8 eV) the XPS peak characteristic of Cr^{3+} in Cr3–Cr6 showed a shift to lower BE indicating the presence of an interaction between Cr3 and Cr6 phases. Finally it can also be noticed that the surface concentration of Cr is higher than that of La. The presence of some superficial La^{3+} ions facilitates the oxidation of Cr^{3+} to Cr^{6+} and its ulterior stabilisation.

The surface composition atomic ratio ($Cr^{3+}/Cr^{6+} = 1.22$) measured by XPS was ca 9 times lower than the corresponding one, determined using XRD ($Cr^{3+}/Cr^{6+} =$

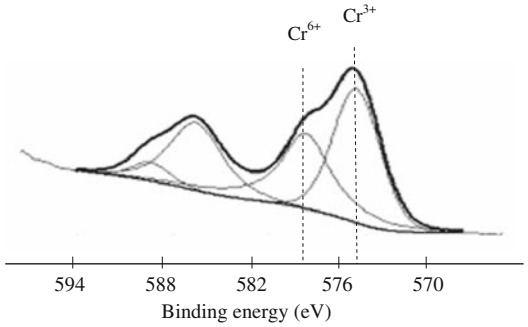

Fig. 3 Cr_{2p} XPS spectrum of 86% Cr3–14% Cr6 catalyst

10.95), indicating that there is a significant enrichment of the surface with Cr^{6+} oxide species. These surface active chromium species is expected to play an important role in methane combustion.

3.4 Catalytic Activity

The Lanthanum–chromium mixed oxides powders prepared in oxygen or hydrogen have been studied as catalysts in methane combustion under equal reaction conditions. Catalytic tests were performed in a temperature range of 300–800 °C at GHSV of 8,000 h^{-1}. For comparison La_2O_3, $LaCrO_3$ (A and B) and La_2CrO_6 were also tested. Results are given in Fig. 4 where the calculated methane conversion as a function of temperature is shown.

The activity of lanthanum chromium oxides catalysts which are related both to the nature of the phases and BET surface area (Table 1) decreased in the order La_2O_3 > 94%Cr3–6%La_2O_3 > Cr3-A > Cr6 > 86%Cr3–14%Cr6 > Cr3-B. However, Cr3–Cr6 and Cr6 activity curves intersected at ca. 760 °C while those of 94%Cr3–6%La_2O_3 and Cr3-A intersected at ca. 725 °C. The catalytic

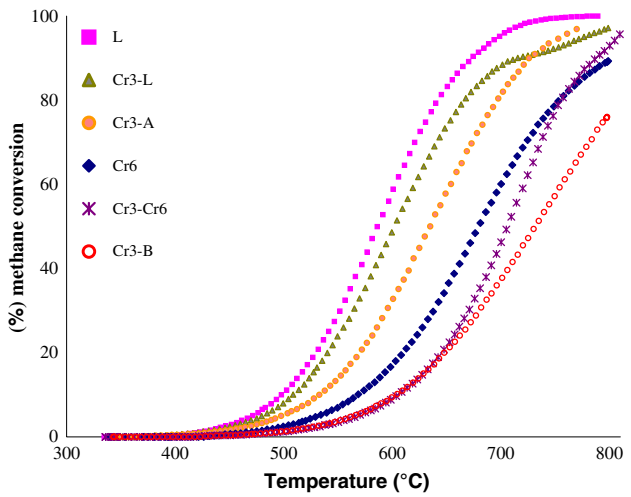

Fig. 4 % methane conversion as a function of temperature on La_2O_3, 94% Cr3–6%La_2O_3, Cr3-A, Cr6, 86% Cr3–14% Cr6 and Cr3-B

activity of Cr3–La_2O_3 catalysts, prepared from precursors heated in hydrogen was found to be better than that of Cr3–Cr6 (obtained after calcination of the precursor in oxygen). The noticeable increase in methane conversion may be ascribed to the presence of La_2O_3, even at low content, in the catalyst while the decrease of catalytic performance can be attributed mainly to the presence of Cr6 phase which has the greatest oxygen mobility at higher temperature. Nevertheless, La_2O_3 and Cr3-L catalysts, which were not reducible in our TPR conditions (1% H_2 in He; $25 \leq T \leq 950$ °C) were found to be more active in methane combustion than Cr6 at all temperatures used. Our results are in agreement with those obtained by Fierro et al. [35] which reported that La_2O_3 showed better catalytic performances in methane combustion than perovskites.

To illustrate clearly the effect of Cr^{3+}/Cr^{6+} and Cr^{3+}/Cr^{5+} in lanthanum–chromium oxides catalysts on the catalytic activity, methane catalytic combustion was investigated by using in situ XRD. The investigation showed that Cr6 phase (ICDD 26-817) is formed progressively (Cr3–Cr6) by exposing 94%Cr3–6%La_2O_3 catalyst to the reactants; 1%CH_4 and 4%O_2, N_2 balance (Fig. 5a). The presence of Cr6 was accompanied with a slight suppression of activity increase between 700 and 740 °C (Fig. 4). However, at $T > 750$ °C Cr6 transformed in turn into Cr4 (ICDD 36-93) (Fig. 5a). The latter was found to be responsible of catalytic activity increase in the 750–800 °C temperatures interval (Fig. 4). During cooling at ca. 725 °C, the disappearance of Cr4 features and the simultaneous appearance of XRD patterns characteristic of Cr6 indicated that the Cr4 to Cr6, transformation occurred too (Fig. 5b). The catalytic activity of the resulting phase composition Cr3–Cr6 was found as expected (Fig. 4) to be lower than that observed for the Cr3–La_2O_3 (Fig. 6).

These results seem to suggest that the Cr6 oxygen species interacted with methane and led to the formation of Cr4 metastable phase ($Cr^{6+} \rightarrow Cr^{3+}$) although the oxygen-to-methane ratio in the stream was 4.

The same experiments performed with Cr3-L under oxygen only (both during heating and cooling) in 25–800 °C temperature interval revealed the formation of Cr6 phase too but not of the Cr4 phase (Fig. 7 a, b).

In order to ascertain both the reversibility of the Cr6 ↔ Cr4 transitions, under reactants, and the suppression of activity increase at high temperature (>700 °C) due the presence of Cr6 phase we have prepared and tested, under the same operating conditions as above, two additional catalysts with higher amounts of Cr6 phase; 60%Cr3–40%Cr6 and 40%Cr3–60%Cr6. The conversion profiles of methane versus reaction temperature are displayed in Fig. 6. For $T < 720$ °C similar activity trends to that of Cr6 were found for 60%Cr3–40%Cr6 and 40%Cr3–60% Cr6 catalysts. The results are consistent with and

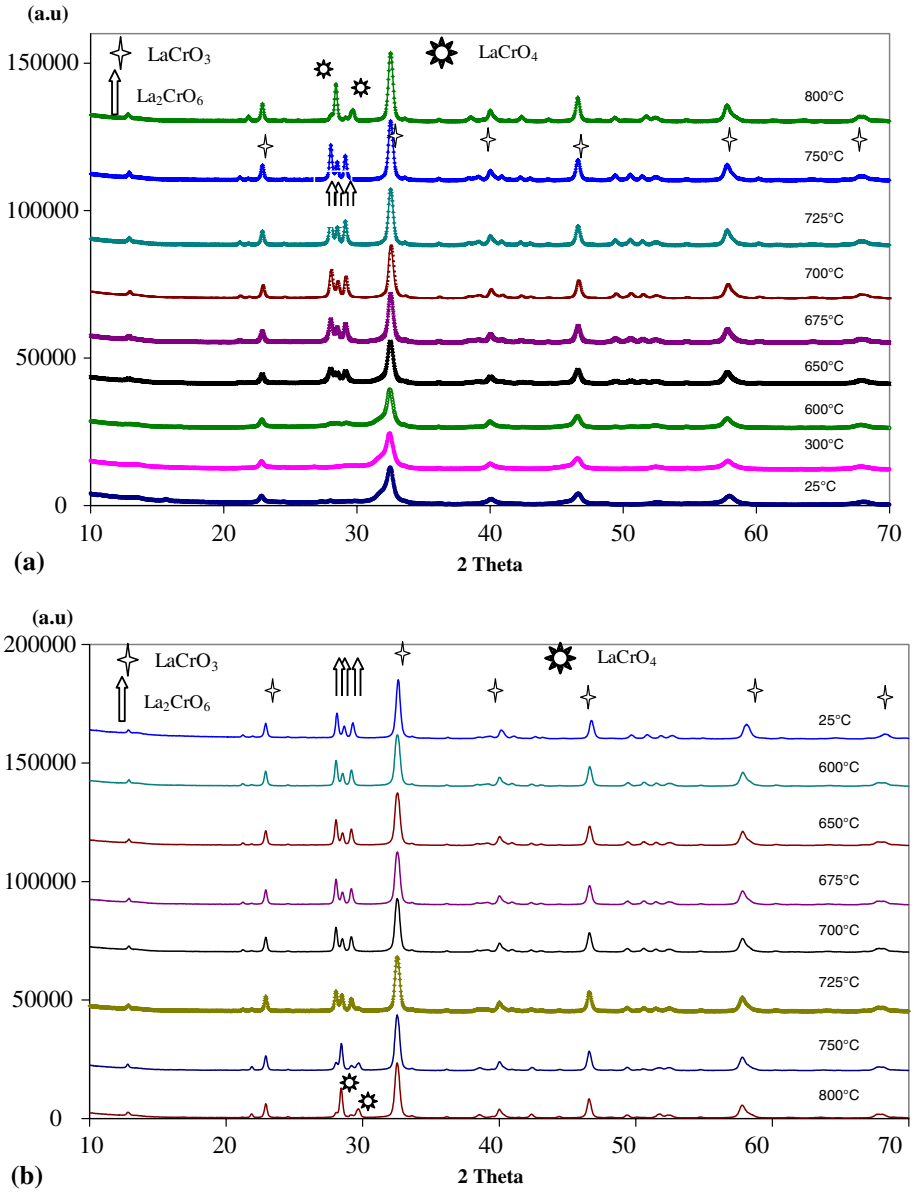

Fig. 5 In situ X-ray diffraction patterns of 94% Cr3–6% L catalyst activated under reactants from ambient temperature to 800 °C, **a** during heating, b while cooling

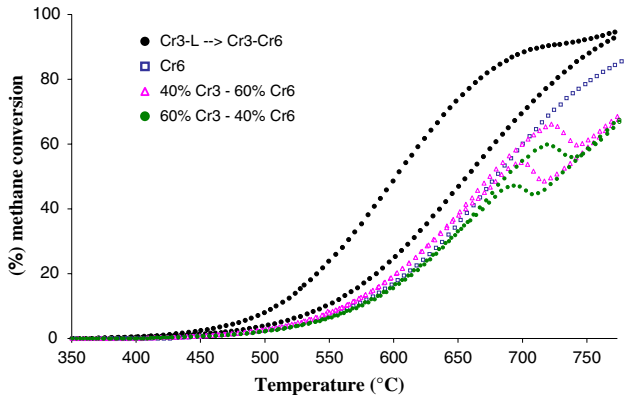

Fig. 6 % methane conversion as a function of temperature on Cr3-L → Cr3–Cr6, Cr6, 40% Cr3–60% Cr6 and 60% Cr3–40% Cr6

parallel the catalyst composition. Catalytic data showed a continuous increase in methane conversion with temperature up to ca. 725 °C, for both 60%Cr3–40%Cr6 and 40%Cr3–60%Cr6 samples, and then a drop in the temperature range of 725–750 °C. The drop in methane conversion was found to be more important for catalysts with low contents of Cr6 phase. The activity increased again when Cr6 → Cr4 transition occurred ($T > 750$ °C). During cooling at ca. 710 °C the back transition Cr4 → Cr6 occurred too. The hysteresis loops, characteristic of the catalytic performances of both 60%Cr3–40%Cr6 and 40%Cr3–60%Cr6 catalysts, during heating and cooling under reactants (Fig. 6) showed that while direct and back Cr4 ↔ Cr6 transition temperatures were unaffected by Cr6 content in the samples, the methane

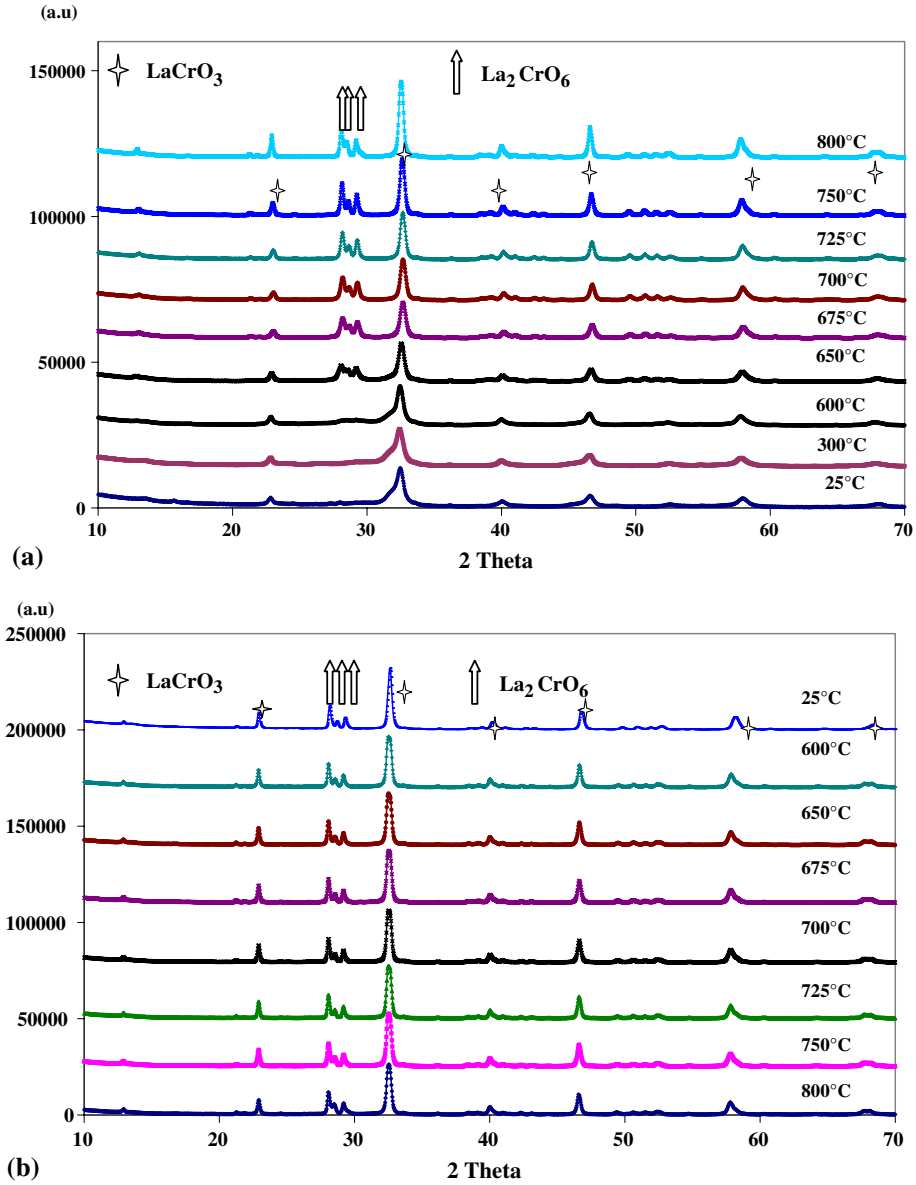

Fig. 7 In situ X-ray diffraction patterns of 94% Cr3–6% L activated under oxygen from ambient temperature to 800 °C, **a** during heating, **b** while cooling

conversion was strongly modified in the same temperature interval.

These results can be explained in terms of the cooperative effects of Cr3 and Cr6 phases at low temperatures (<725 °C) and Cr3 and Cr4 phases at high temperatures (>750 °C) whose relative concentration determines the oxygen activation capability and hence their reactivity for the oxidation of methane. It is worth nothing that under the same operation conditions pure Cr6 phase did not undergo any phase transition into Cr4.

4 Conclusions

Several lanthanum–chromium oxides have been synthesised using a combination of co-precipitation and hydrothermal methods followed by calcinations at high temperatures. Different chromium oxidation states Cr^{3+}/Cr^{6+} and Cr^{3+}/Cr^{5+} were obtained depending on heating atmospheres used (oxygen, hydrogen or reactants). TPR results evidenced a highest mobility of surface oxygen species for Cr3–Cr6 and Cr6 catalysts.

Investigation of the La–Cr–O catalysts, under working conditions, with in situ XRD (ISXRD) technique has given particular insight into the structure, phase composition and chromium oxidation states. The present study provided not only an understanding of the influence of surface Cr species on methane activation but also showed that at high temperatures Cr6 transformed into $LaCrO_4$ metastable phase which cannot be evidenced during conventional catalytic experiments. The presence of Cr4 phase was associated with an interaction of methane with Cr6.

References

1. Peña MA, Fierro JLG (2001) Chem Rev 101(no 7):1981
2. Nitadori T, Misono M (1985) J Catal 93:459
3. Ferri D, Forni L (1998) Appl Catal B Environ 16:119
4. Kaddouri A, Ifrah S, Gelin P (2007) Catal Lett 119(no 3/4):237
5. Fino D, Russo N, Saracco G, Specchia V (2003) J Catal 217:367
6. Kremenic G, Nieto JML, Tascon JMD, Tejuca LGJ (1985) Chem Soc Faraday Trans 1(81):939
7. Iwamoto M, Yoda Y, Yamazoe N, Seiyama T (1982) J Phys Chem 72:2564
8. Shu J, Kagliaguine S (1998) Appl Catal B Environ 16:L303
9. Seyama T (1992) Catal Rev Sci Eng 34:281
10. Yamazoe N, Teraoka Y (1990) Catal Today 8:175
11. Russo N, Fino D, Saracco G, Specchia V (2005) J Catal 229(no 2):459
12. Ifrah S, Kaddouri A, Gelin P, Bergeret G (2007) Catal Comm 8(no 12):2257
13. Fino D, Russo N, Saracco G, Specchia V (2003) J Catal 217(no 2):367
14. Wisvanathan T (1993) In: Tejuca LG, Fierro JLG (eds) Properties and applications of perovskites-type oxides. Marcel Dekker, New York, p 271
15. Swamy CS, Christopher J (1993) In: Tejuca LG, Fierro JLG (eds) Properties and applications of perovskites-type oxides. Marcel Dekker, New York, p 343
16. Sinquin G, Petit C, Libs S, Hindermann JP, Kiennemann A (2000) Appl Catal B Environ 27:105
17. Schneider R, Kieβling D, Wendt G (2000) Appl Catal B Environ 28:187
18. McCarthy JG, Wise H (1990) Catal Today 8:231
19. Tejuca LG, Fierro JLG, Tascon JMD (1989) Structure and reactivity of perovskites-types oxides. In: Eley DD, Pines H, Weisz PB (eds) Advances in catalysis, vol 36. Academic Press, New York, p 237
20. Arai H, Yamada T, Eguchi K, Seiyama T (1986) Appl Catal 26:265
21. Maurin I, Barboux P, Lassailly Y, Boilot JP, Vilain F, Dordor P (2001) J Solid State Chem 160(1):123
22. Ritter C, Ibarra MR, De Teresa JM, Algarabel PA, Marquina C, Blasco J, Garcia J, Oseroff S, Cheong SW (1997) Phys Rev B 56(14):8902
23. Mitchell JF, Argyriou DN, Potter CD, Hinks DG, Jorgensen JD, Bader SD (1996) Phys Rev B 54(9):6172
24. De Silva PSIPN, Richards FM, Cohen LF, Alonso JA, Martinez-Lope MJ, Casais MT, Thomas KA, MacManus-Driscoll JL (1998) J Appl Phys 83(1):394
25. Saracco G, Scibilia G, Iannibello A, Baldi G (1996) Appl Catal B Environ 8:229
26. Rosso I, Saracco G, Specchia V, Garrone E (2003) Appl Catal B Environ 40:195
27. de Collongue B, Garbowski E, Primet M J Chem Soc Farad Trans 87(15): 2493
28. Topsoe H (2003) J Catal 216:155
29. Banares MA (2005) Catal Today 100:71
30. Moggridge GD, Rayment T, Lambert RM (1992) J Catal 134:242
31. Ifrah S, Kaddouri A, Gélin P, Garbowski E, Leonard D (2006) Stud Surf Sci Catal 162:705
32. Berjoan R, Traverse JP, Coutures JP (1973) Rev Chim Minér 10:309
33. Teraoka Y, Yoshimatsu M, Yamazoe N, Seiyama T (1984) Chem Lett: 893
34. Seyama T (1992) Catal Rev Sci Eng 34:281
35. Milt VG, Spretz R, Ulla MA, Lombardo EA, Garcia Fierro JL (1996) Catal Lett 42:57